Modelling Weld Point Location in High-frequency Electric Resistance Welding

Daniele D. G. Calista [a], Greg. R. Lehnhoff [b], Prof. Patricio F. Mendez [a]
[a]University of Alberta, Edmonton, Canada; [b] InterPro Pipe and Steel, Regina, Canada

Background

High-frequency electric resistance welding (HFW) is a common process used to fabricate seamed tubular goods. The process is fast, autogenous, and uses alternating current (AC) Joule heating to heat steel sheets prior to welding the edges together.

Despite its wide use, practitioners and engineers have limited ability to understand or design welding procedures. One key aspect of the process is its ***process-dependent weld point***, which has been repeatedly observed to vary with changing process conditions, and ***is related to defect generation.***

Today, practitioners commonly assume the weld point is fixed by mill geometry, and engineers commonly conduct simulations with fixed weld point assumptions.

Goal and objectives

Goal: This work is a part of a larger effort to provide industry practitioners with quick, yet accurate, mathematical tools to select weld parameters without trial-and-error testing or tailored numerical simulation experience.

Primary objective: ***Develop*** and ***validate*** a new ***framework*** for ***predicting*** the ***weld point location*** in HFW.

Secondary objective: ***Understand*** the ***connection*** between ***parameters*** and ***weld defect generation.***

Key methods and governing equations

- Simplified approach using minimally representative framework to establish concise mathematical relationships.
- Material properties are accounted for using a constant effective property heuristic that has been proven sufficient for welding and AM processes (integral-average).

Temperature field:

- Due to symmetry, the interfaces are modelled as independent semi-infinite slabs with a volumetric AC-Joule heat source.
- AC density is governed by the skin depth δ_e, a characteristic depth that describes how current concentrates to the weld interface in HFW.
- AC-Joule heating is governed by the power depth δ_P.
- The 2-D temperature field $T(x,y)$ is governed by:

$$0 = k\frac{\partial^2 T}{\partial y^2} - \rho c U \frac{\partial T}{\partial x} + q_0''' \exp\left(-\frac{y}{\delta_P}\right)$$

Explicit full solution reported in:
D. D. G. Calista and P. F. Mendez, "Heat transfer in high-frequency electric resistance welding: Scaling analysis of isotherm location under a moving AC-Joule heat source," Int J Heat Mass Transf, vol. 271, p. 129362, Dec. 2026, doi: 10.1016/j.ijheatmasstransfer.2026.129362.

Material ejection:

- In HFW, there are Lorentz-forces that expel any material that reaches melting. This removal of material at a critical temperature (i.e. melting) is modelled as *ablation.*
- The depth of ablation $D(x)$ is governed by the transverse velocity of the ablated interface $U_a(x)$:

$$D(x) = \int_0^{x_w} U_a(x)\mathrm{d}x$$

$$0 = k\frac{\partial^2 T}{\partial y^2} - \rho c U \frac{\partial T}{\partial x} + \rho c U_a(x) \frac{\partial T}{\partial y}$$

$$q_0''' \delta_P = -k \left.\frac{\partial T}{\partial y}\right|_{y=0} + \rho i_{sl} U_a(x)$$

Explicit full solution reported in:
P. F. Mendez and U. Prisco, "Depth and Velocity of Ablation Under a Constant Heat Flux," *ASME Journal of Heat and Mass Transfer*, vol. 147, no. 8, Aug. 2025, doi: 10.1115/1.4068348.

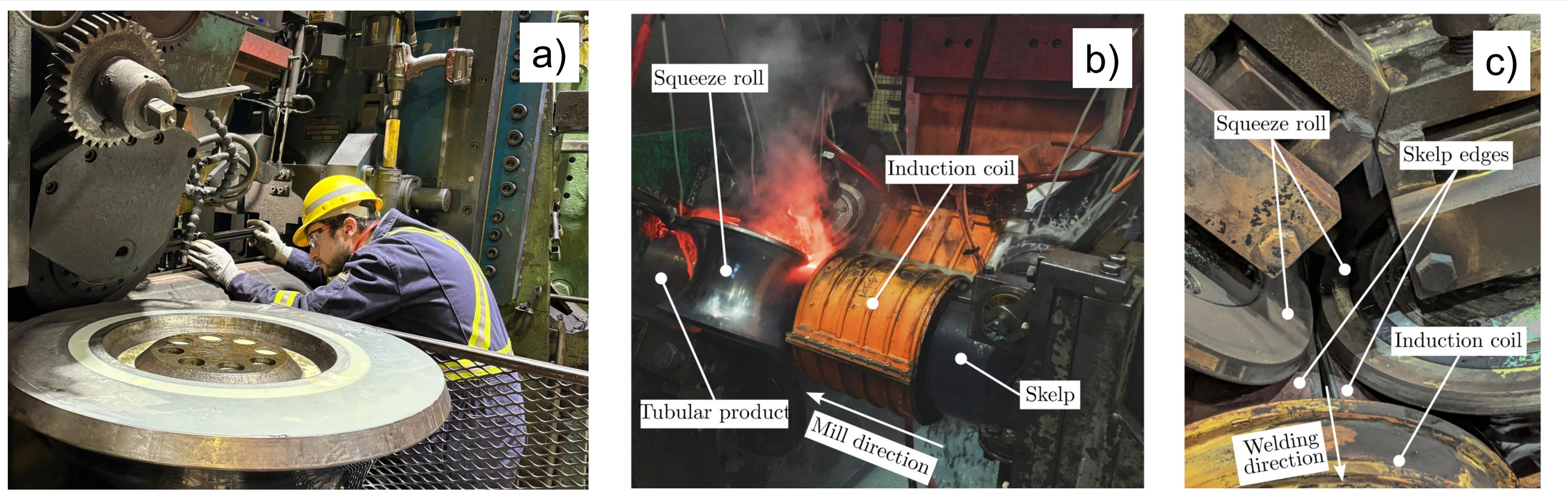

Figure 1 – A full-scale HFW weld box configuration on an induction pipe mill. (b) The mill in operation (on-state) welding skelp from right to left. (c) The mill in a static (off-state) condition, clearly showing the convergent "vee" geometry formed by the skelp edges prior to the point of welding.

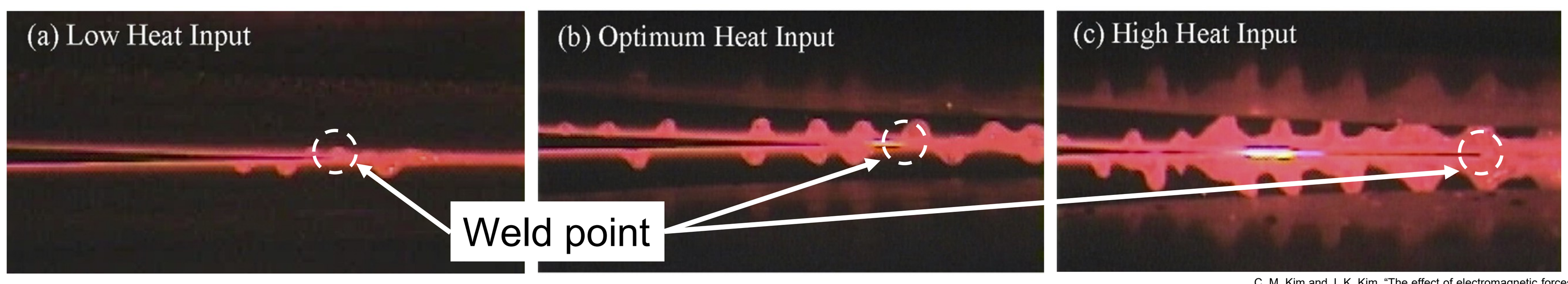

Figure 2 – *High-speed videography of the HFW weld point at different heat inputs (a-c).*

C. M. Kim and J. K. Kim, "The effect of electromagnetic forces on the penetrator formation during high-frequency electric resistance welding," *J Mater Process Technol*, vol. 209, no. 2, pp. 838–846, Jan. 2009, doi: 10.1016/J.JMATPROTEC.2008.02.079.

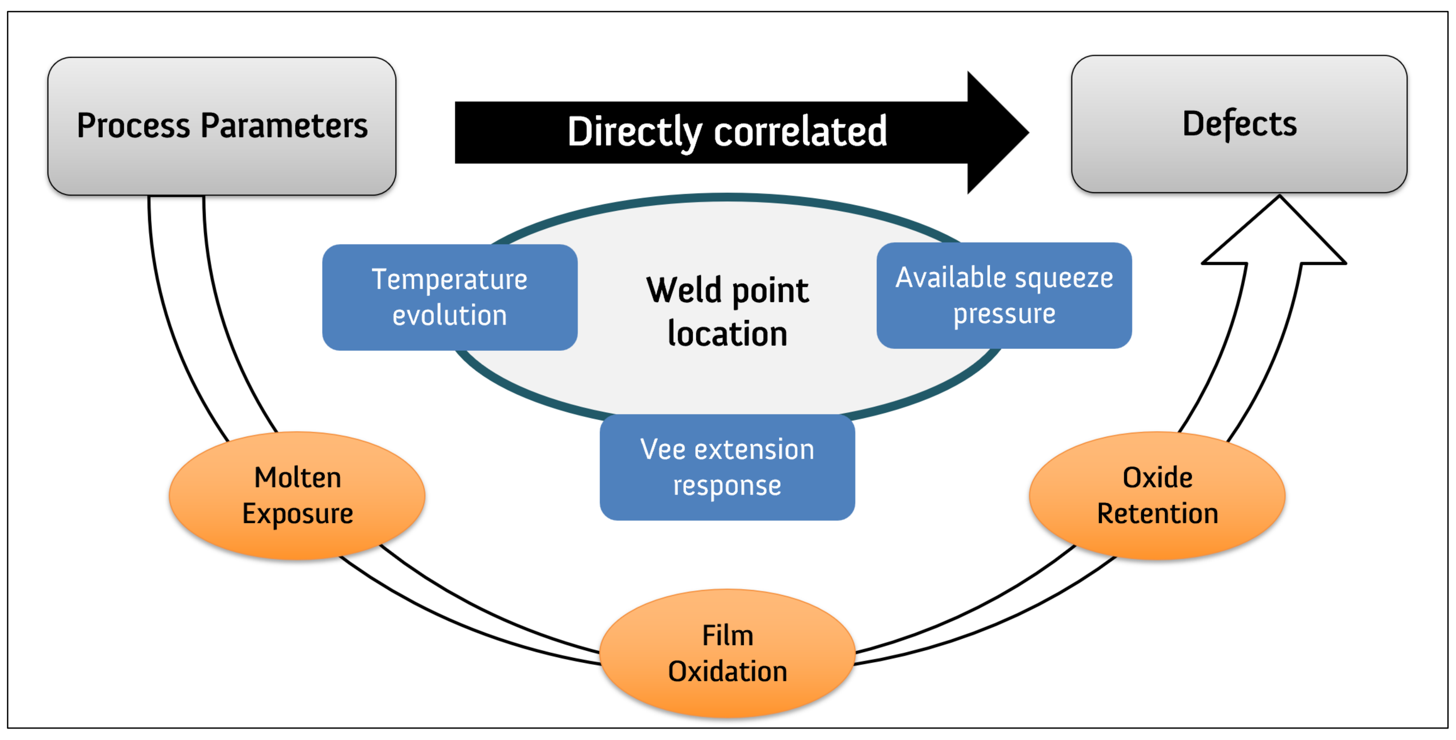

Figure 3 – *The relationship between general process parameters, key phenomena in HFW (orange), the central physical effects (blue), and the key process variable that controls the process (weld point location).*

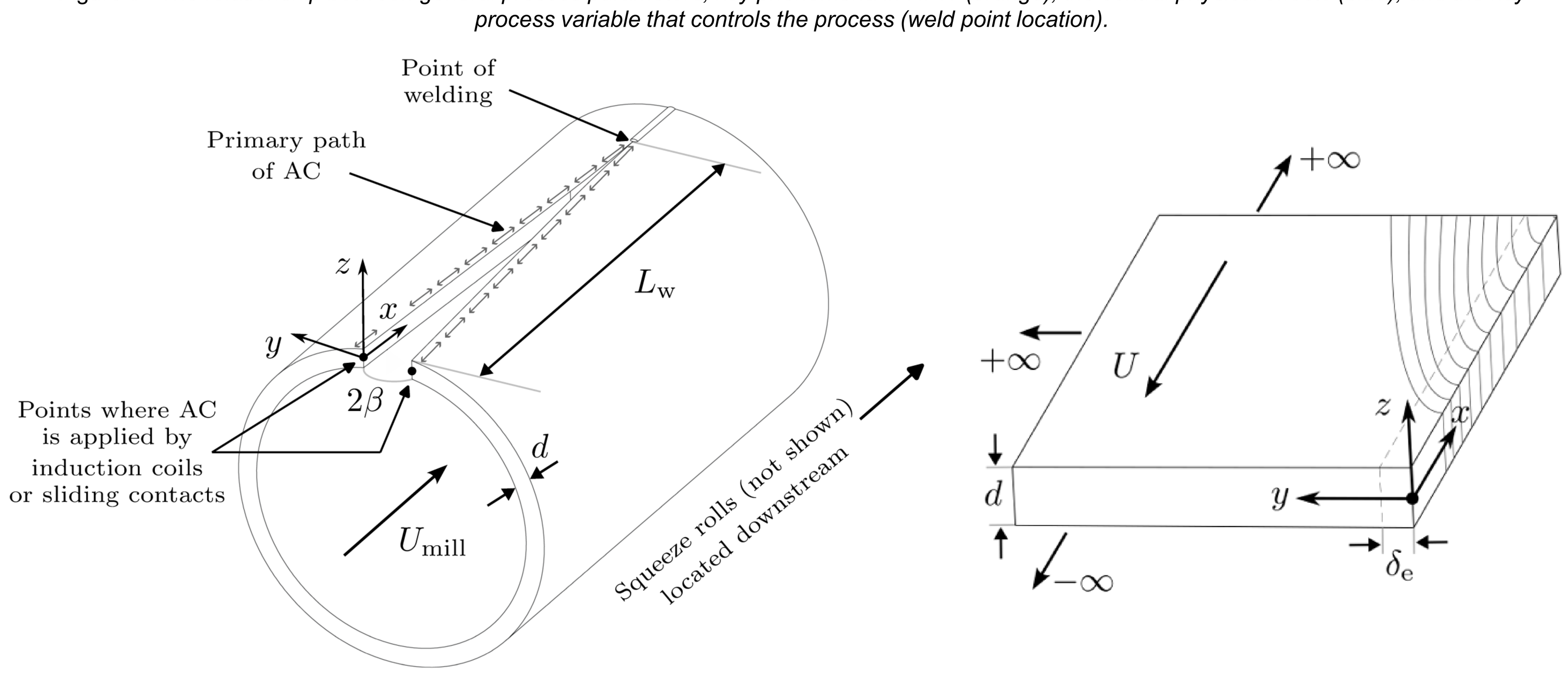

Figure 4 – *Simplified schematic of the HFW process: (left) the key parameters in the weld vee; (right)* Eulerian domain of analysis for a substrate of thickness d, containing an AC-Joule heat source translating at velocity (U) with characteristic skin depth (δ_e). The heat source is concentrated near the $x-z$ plane and considered uniform in the z-direction, resulting in the 2-D isotherms shown.

Model development

- To define the weld vee, **four** concepts must be defined:
  1. The point where melting initiates: x_m
  2. A fixed point of geometrical convergence: x_g
  3. The vee extension between x_g and the actual weld point x_w: L_{ext}
  4. The apparent weld point "depth" relative to the weld interface: y_w

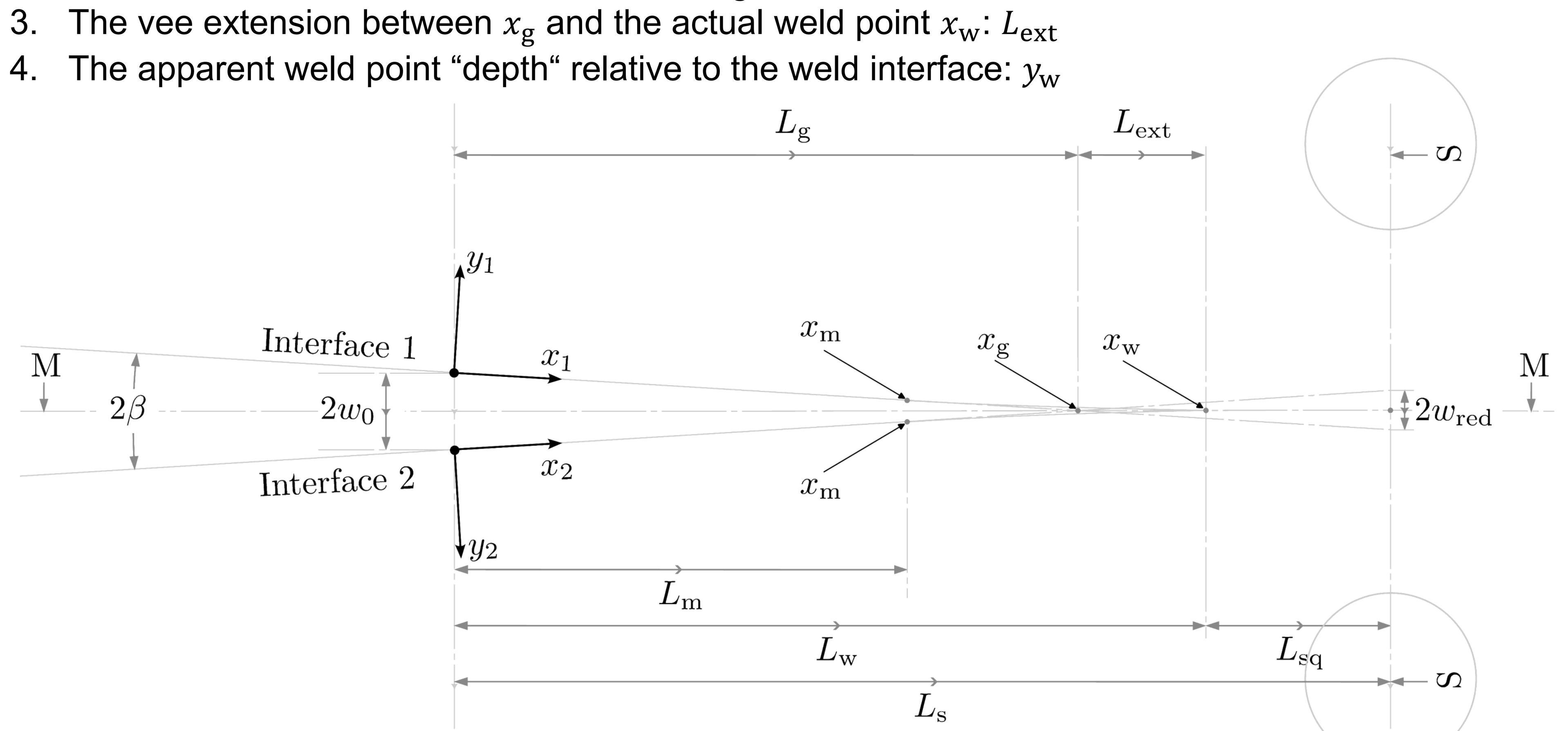

Figure 5 – *Notation of the weld zone (or vee) in HFW, where all lengths are to scale. The two weld interfaces are modelled with their own coordinate systems due to symmetry.*

- To establish the **link** between **process parameters** and **weld point** location, we must define three equations to **solve for three unknowns in space**: $\{x_m, x_w, y_w\}$
  1. Temperature field
     $\Delta T_m = \Delta T|_{y=0}(x_m, x_w, U, \delta_e, q, d, \alpha, k)$
  2. Ablation depth (transient ejection of melt)
     $y_w = D_w = D(x_m, x_w, \Delta T_m, q, U, \delta_e, d, \alpha, k, i_{sl})$
  3. Physical constraints (interface conjoining)
     $y_w = \mathrm{M}(x_w) = \tan(\beta)(x_w - L_g)$

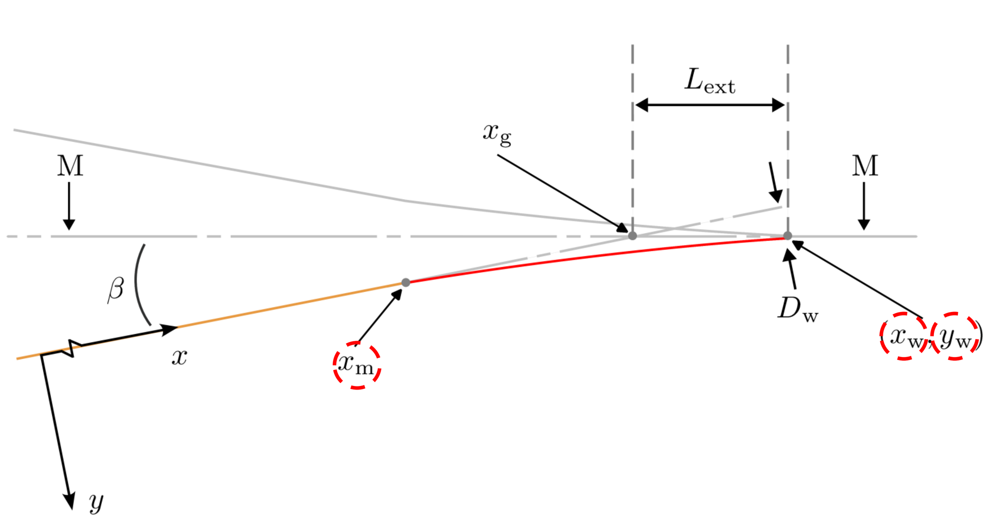

Figure 6 – *Schematic of the HFW weld zone depicting the interaction of the three critical unknowns in the proposed vee length model. Note diagram is not to scale.*

Model validation and insights

- Data from two independent full-scale mill trials was used to validate the model.

[1] H. Haga, K. Aoki, and T. Sato, "Welding Phenomena and Welding Mechanisms in High Frequency Electric Resistance Welding - 1st Report," Weld J, vol. 59, no. 7, pp. 208–212, Jul. 1980.

[2] P. F. Scott, "A Study of the Key Parameters of High Frequency Welding," 1996.

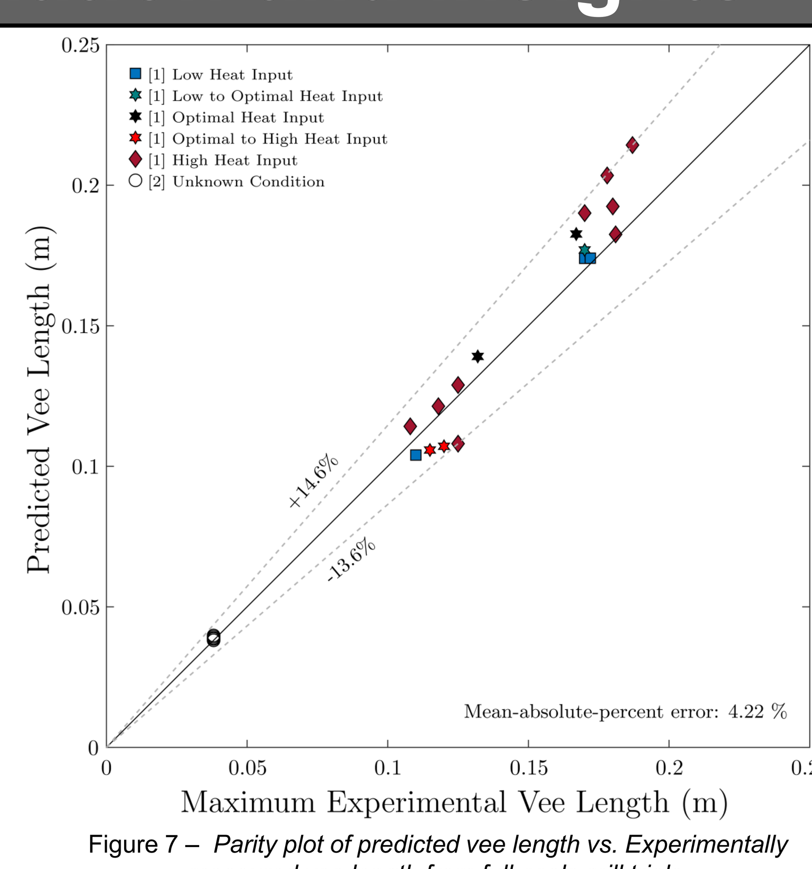

Figure 7 – *Parity plot of predicted vee length vs. Experimentally measured vee length from full-scale mill trials.*

- Further insights into the process can be obtained by plotting the resultant weld point (x_w) and melting onset point (x_m) versus normalized heat input or AC magnitude (I)

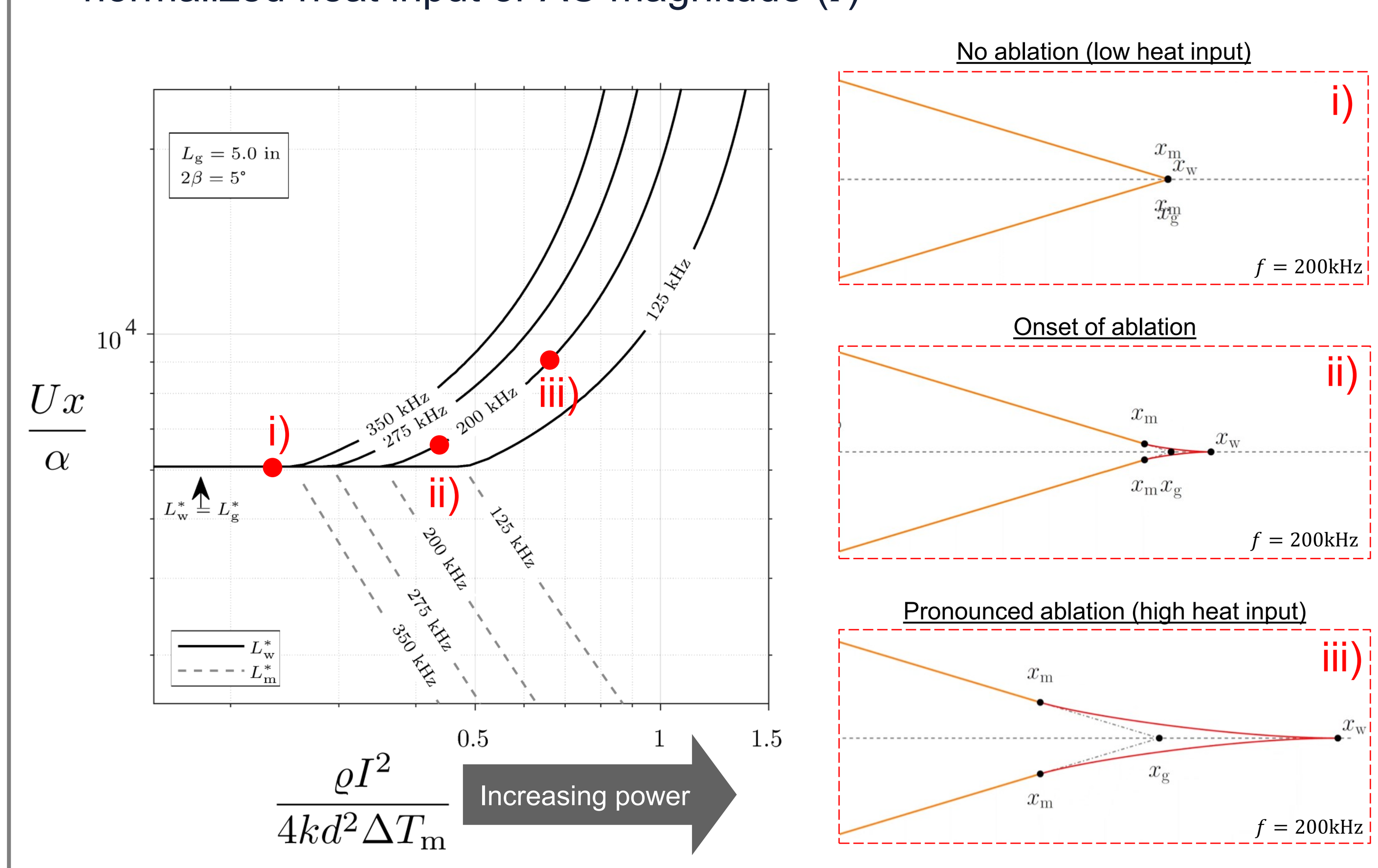

Figure 8 – *Plot of normalized space in x-direction versus normalized power or current. The resulting vee shapes are highlighted for three different cases. Schematics are not to scale.*

Conclusions

1. The weld point location in HFW is a process dependent magnitude that is a function of heat input.
2. A model is presented, and validated, to predict the weld point location in HFW. The model is not empirically fitted, and is applicable for a wide range of alloys and weld parameters.
3. The vee length is affected by process parameters including power, AC frequency, and mill speed. This contrasts a common assumption that mill geometry is the determining factor, but matches previous observations using high-speed videography.
4. Weld parameters dictate the vee length through their direct influence on melting initiation and ablation depth.

Acknowledgments

This work was supported by InterPro Pipe and Steel, the Natural Sciences and Engineering Research Council of Canada (NSERC) under Alliance Grant No. 602383, and the American Welding Society Foundation, and an AWS Research Fellowship.